



LJMU Research Online

Prang, TC, Ramirez, K, Grabowski, M and Williams, SA

Ardipithecus hand provides evidence that humans and chimpanzees evolved from an ancestor with suspensory adaptations

<http://researchonline.ljmu.ac.uk/id/eprint/14521/>

Article

Citation (please note it is advisable to refer to the publisher's version if you intend to cite from this work)

Prang, TC, Ramirez, K, Grabowski, M and Williams, SA (2021) Ardipithecus hand provides evidence that humans and chimpanzees evolved from an ancestor with suspensory adaptations. *Science Advances*, 7 (9). pp. 1-13. ISSN 2375-2548

LJMU has developed [LJMU Research Online](#) for users to access the research output of the University more effectively. Copyright © and Moral Rights for the papers on this site are retained by the individual authors and/or other copyright owners. Users may download and/or print one copy of any article(s) in LJMU Research Online to facilitate their private study or for non-commercial research. You may not engage in further distribution of the material or use it for any profit-making activities or any commercial gain.

The version presented here may differ from the published version or from the version of the record. Please see the repository URL above for details on accessing the published version and note that access may require a subscription.

For more information please contact researchonline@ljmu.ac.uk

<http://researchonline.ljmu.ac.uk/>

ANTHROPOLOGY

Ardipithecus hand provides evidence that humans and chimpanzees evolved from an ancestor with suspensory adaptations

Thomas C. Prang^{1*}, Kristen Ramirez^{2,3,4}, Mark Grabowski^{5,6}, Scott A. Williams^{2,7,8}

The morphology and positional behavior of the last common ancestor of humans and chimpanzees are critical for understanding the evolution of bipedalism. Early 20th century anatomical research supported the view that humans evolved from a suspensory ancestor bearing some resemblance to apes. However, the hand of the 4.4-million-year-old hominin *Ardipithecus ramidus* purportedly provides evidence that the hominin hand was derived from a more generalized form. Here, we use morphometric and phylogenetic comparative methods to show that *Ardipithecus* retains suspensory adapted hand morphologies shared with chimpanzees and bonobos. We identify an evolutionary shift in hand morphology between *Ardipithecus* and *Australopithecus* that renews questions about the coevolution of hominin manipulative capabilities and obligate bipedalism initially proposed by Darwin. Overall, our results suggest that early hominins evolved from an ancestor with a varied positional repertoire including suspension and vertical climbing, directly affecting the viable range of hypotheses for the origin of our lineage.

INTRODUCTION

The morphology and inferred positional behavior of the last common ancestor (LCA) of humans, chimpanzees, and bonobos (hereafter, “LCA”) are critical for understanding the evolution of hominin bipedalism (1–5). Numerous adaptive explanations for bipedalism rely on an understanding of our place in nature. The recognition that humans are closely related to African apes influenced the range of possible explanations for bipedalism by raising questions about the kind of ancestor from which the human *bauplan* was derived (1). Keith (6) established the hypothesis that human postcranial anatomy was derived from an orthograde ancestor, later interpreted as a “brachiating” ancestor (7), by highlighting the aspects of trunk and limb anatomy shared among humans and other hominoids.

The morphology of the highly dexterous human hand, with its intrinsically elongated first ray (pollex or thumb), shortened metacarpals and nonpollical digits, and hypertrophied thenar muscles, contrasts sharply with that of suspensory adapted anthropoid primates (8–10). The most suspensory hominoids, cercopithecoids, and platyrrhines tend to display a reduced pollex and narrow, elongated nonpollical rays. For example, *Pan*, *Pongo*, and *Colobus* have a markedly reduced thumb, and *Ateles* and *Brachyteles* have entirely lost an external thumb (8, 11). In these features, humans were argued to more closely resemble cercopithecoid primates than hominoids (10–12). The recognition that human and suspensory hominoid hands are specialized in seemingly divergent directions influenced the development of an alternative hypothesis in which humans evolved from

a quadrupedal, cercopithecoid-like ancestor instead of a suspensory, hominoid-like one (10–12).

Detailed comparative research demonstrated that the hands of humans and cercopithecoids are only superficially similar in morphology (13–15). For example, although humans have an intrinsically elongated thumb compared to most hominoids, the lengths of the nonhuman hominoid pollical metacarpal and phalanges are not reduced relative to their body size (13). Furthermore, humans and other hominoids share an intra-articular meniscus on the ulnar side of the wrist responsible for isolating the ulnar styloid process (14, 16). Humans also share with chimpanzees, bonobos, and gorillas the fusion of the os centrale and scaphoid (1, 13, 15), which increases midcarpal joint stability and decreases joint stress (1). The shared aspects of hand and wrist morphology among humans and nonhuman hominoids, especially the African apes, supported Keith’s hypothesis (6) that humans evolved from a hominoid-like ancestor.

However, later discoveries of Miocene hominoid fossils preserving primitive postcranial morphology relative to extant hominoids suggested that the anatomical correlates of below-branch suspension might have evolved multiple times throughout hominoid evolutionary history (2–4, 17, 18). Few Miocene hominoids have traits that reflect the undisputed use of hominoid-like suspensory locomotion (19), with the potential exception of *Hispanopithecus laietanus* (18) and *Danuvius guggenmosi* (20). For example, the Miocene fossil hominoids *Sivapithecus* and *Pierolapithecus* have dorsally oriented articular surfaces of their manual proximal phalanges, indicating the habitual use of extended metacarpophalangeal (MCP) joints in palmigrade quadrupedalism (21).

The hand of the early Pliocene hominin partial skeleton ARA-VP-6/500 attributed to *Ardipithecus ramidus* has been argued to support the hypothesis of a nonsuspensory LCA (2–4, 22). The initial analysis of the ARA-VP-6/500 hand concluded that *Ar. ramidus* had none of the adaptations associated with forelimb-dominated suspension present among extant hominoids (2–4). Instead, the hand of *Ar. ramidus* was argued to be reminiscent of more “generalized” (in some ways monkey-like) Miocene hominoids such as *Ekembo* and *Pierolapithecus*. If *Ar. ramidus* did not have a suspensory-adapted

¹Department of Anthropology, Texas A&M University, College Station, TX 77843, USA. ²New York Consortium in Evolutionary Primatology, New York, NY 10024, USA. ³Department of Anthropology, CUNY Graduate Center, New York, NY 10016, USA. ⁴Office of Medical Education, NYU Grossman School of Medicine, New York, NY 10016, USA. ⁵Research Centre in Evolutionary Anthropology and Palaeoecology, Liverpool John Moores University, Liverpool, UK. ⁶Centre for Ecology and Evolutionary Synthesis, Department of Biosciences, University of Oslo, Oslo, Norway. ⁷Center for the Study of Human Origins, Department of Anthropology, New York University, New York, NY 10003, USA. ⁸Evolutionary Studies Institute, University of the Witwatersrand, Private Bag 3, Wits 2050, Johannesburg, South Africa.
*Corresponding author. Email: prang@tamuedu

hand and instead had a more generalized morphology, then human hand morphology may be less derived than that of chimpanzees and bonobos relative to the LCA (2, 22). In this case, the distinctive pollical to nonpollical ray proportions of modern humans would be considered an exaptation, rather than an adaptation, useful for manipulation and tool use (23, 24) since it originated in the context of Miocene hominoid arboreal quadrupedal locomotion and feeding behavior (22, 25).

Thus, inferences about the positional behavior of fossil hominoids and hominins have contributed to a more recent alternative hypothesis, which proposes that each extant hominoid lineage was independently derived for suspensory posture and locomotion from more generalized ancestors with “cautious climbing” adaptations (2–4). This alternative hypothesis is a refinement of Straus’ earlier hypothesis (10, 11), in that it concedes the phylogenetic position of humans as the sister taxon of chimpanzees and bonobos within the great ape clade, combined with suggestions that cautious climbing, not suspension, explains the locomotor anatomy of hominoids (16, 26).

Here, we test the hypothesis that hominins evolved from an ancestor that lacked adaptations for below-branch suspension using metric data from a large and diverse sample of extant primates and fossil hominins with special emphasis on the hand of *Ar. ramidus*. We combine standard morphometric analyses with phylogenetic comparative methods that allow us to reconstruct the adaptive landscape of hominin hand evolution, placing fossil taxa within shared selective regimes. Species in a selective regime share a common selective factor, e.g., positional behavior, where regime shifts imply evolution toward new adaptive optima brought on by a change in selection. First, we evaluate the morphometric affinities of the *Ar. ramidus* hand and show that it is most similar to chimpanzees, bonobos, and orangutans among a sample of 53 anthropoid primate species. Second, we reconstruct the evolution of the hominin hand and show that *Ar. ramidus* evolved in a selective regime shared with modern chimpanzees and bonobos to the exclusion of later hominins. Overall, our results (i) provide a more refined view of the positional behavior of *Ar. ramidus* and the *Homo*-*Pan* LCA, (ii) resolve a long-standing debate about the role of suspension in the ancestry of humans (2–4, 7, 27), and (iii) imply coevolutionary shifts in hominin hand and foot morphology associated with manipulation and obligate bipedality, respectively (23, 24, 28).

RESULTS

Morphometric analyses

To evaluate alternative evolutionary trajectories for the hominin hand, we conducted a principal components analysis (PCA) on 26 logged geometric mean-standardized measurements of metacarpals and phalanges preserved in the ARA-VP-6/500 fossil [first metacarpal (MC1), fifth metacarpal (MC5), third proximal phalanx (PP3), and third intermediate phalanx (IP3)] on the full comparative sample. Our results show that PCA separates extant anthropoid primates according to known differences in hand morphology (Fig. 1 and fig. S1). Hylobatids, *Ateles*, *Brachyteles*, and *Homo* occupy distinct areas of the morphospace associated with their highly specialized hands related to variation in the proportions of the pollical and nonpollical rays. The first principal component (PC1) accounts for 47% of the variance and is primarily associated with the relative lengths of the phalanges and MC5 combined with MC1 variables (table S1 and figs. S2A and S3A). The second principal component (PC2) accounts for

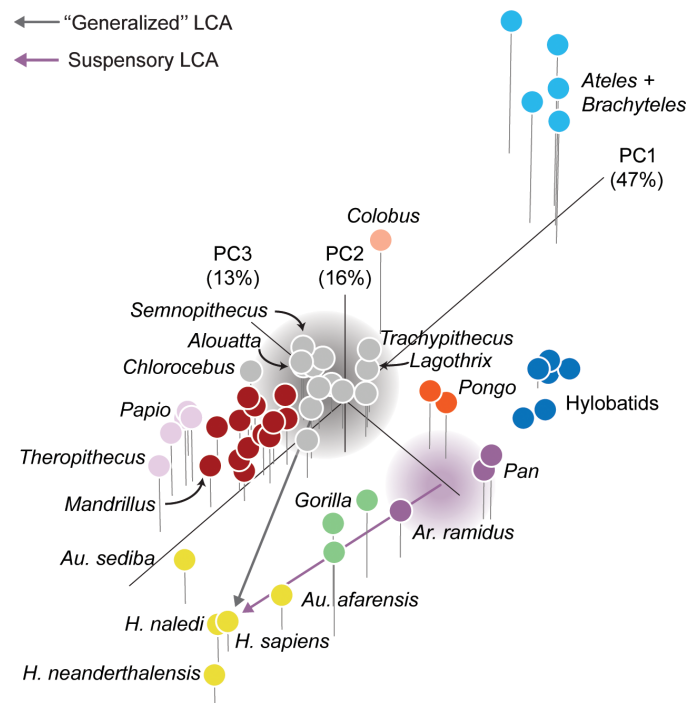


Fig. 1. PCA on 26 logged geometric mean-standardized variables representing between-species variation in hand shape. Each point is a species mean, except among fossil hominins, and colors represent selective regimes identified by SURFACE. *Homo* and *Australopithecus*, gold; *Ar. ramidus*, *P. troglodytes*, and *P. paniscus*, purple; *G. gorilla*, *Gorilla beringei beringei*, and *Gorilla beringei graueri*, light green; *Pongo pygmaeus* and *Pongo abelii*, orange; *Hylobates*, *Hoolock*, *Nomascus*, and *Symphalangus*, blue; *Macaca*, *Mandrillus*, *Cercocebus*, *Cebus*, and *Saimiri*, dark red; *Papio* and *Theropithecus*, pink; *Ateles* and *Brachyteles*, light blue; *Colobus*, tan; remaining platyrrhines, cercopithecins, and colobines, gray. Note that most cercopithecoids and platyrrhines fall along a spectrum of generalized palmigrady to specialized digitigrady. The *Ar. ramidus* and *Au. afarensis* hands fall nearest to a hypothetical evolutionary trajectory from a suspensory, *Pan*-like ancestor instead of a more generalized, monkey-like ancestor. Purple and gray clouds represent hypothetical uncertainties surrounding suspensory *Pan*-like and generalized ancestral morphotypes, respectively.

16% of the variance and is primarily associated with MC1 and MC5 variables (figs. S2B and S3B). The third principal component (PC3) separates hominoids from most other anthropoids with little overlap. PC3 accounts for 13% of the variance and is primarily associated with carpometacarpal joint, MCP joint, and MC1 midshaft dimensions (figs. S2C and S3C).

Ar. ramidus and *Australopithecus afarensis* fall along an evolutionary trajectory from a suspensory LCA when examining the first three PCs together (Fig. 1). The placement of *Au. afarensis* between modern humans and gorillas on PC1 is consistent with a recent re-sampling analysis of hand proportions (29). While *Homo naledi* is nearly indistinguishable from modern humans, *Australopithecus sediba* and *Homo neanderthalensis* are distributed in different directions around the modern human mean, which is consistent with the results of previous studies (30). A multivariate cluster analysis on Euclidean distances between PC scores (unweighted pair group with arithmetic mean) results in a great ape cluster including *Ar. ramidus* nearest to *Pan* and *Pongo* (fig. S4). All other fossil hominins cluster exclusively with modern humans.

To compare the hand of *Ar. ramidus* (ARA-VP-6/500) to the fossil hominoid *H. laietanus* (IPS18800), we conducted a second PCA on 17 logged geometric mean-standardized measurements of metacarpals and phalanges preserved across both hand fossils (MC4, PP3, and IP3). PCA on this modified dataset also separates extant anthropoid primates according to known differences in hand morphology but with less separation among groups since the MC1 is excluded (figs. S5 and S6 and table S2). The *Ar. ramidus* hand (ARA-VP-6/500) falls within the *Pan* distribution along PC1 and PC2 and within the overlapping distributions of *Pan*, *Lagothrix*, and cercopithecoids along PC1 and PC3 (figs. S5A and S6A). The *H. laietanus* hand (IPS8800) is positioned intermediately between *Pongo* and papionins, and within the interquartile range of *Ateles*, along PC2 (figs. S5B and S6B). The *Ar. ramidus* hand is clearly *Pan*-like according to the PCA on the modified dataset, whereas the hand of the great ape *H. laietanus* is positioned intermediately between suspensory taxa (e.g., *Pongo* and *Ateles*) and quadrupedal monkeys. Additional details on PCA loadings (table S2) are outlined in the Supplementary Materials.

To supplement our initial PCA and to offer an additional perspective on the morphometric affinities of the *Ar. ramidus* hand, we conducted discriminant function (DFA) and canonical variates analyses (CVA) on 26 logged geometric mean-standardized measurements of metacarpals and phalanges (MC1, MC5, PP3, and IP3). The DFA correctly classifies 97% of individuals using leave-one-out cross-validation (table S3). All fossil hominin hands were classified as “*Homo*” with a high posterior probability, except the *Ar. ramidus* hand, which was classified primarily as “*Pan*” (table S4). Extant hominoid groups are well separated from each other and from cercopithecoids and platyrrhines in the CVA (fig. S7, A and B, and table S5). The *Ar. ramidus* hand is positioned on the positive end of Canonical Axis 2 (CAN2) within the ranges of *Gorilla*, *Pongo*, and hylobatids and outside the ranges of all other groups (fig. S7A). The A.L. 333 and MH2 fossil hands are classified as *Homo* but are positioned just outside of the range of *Homo sapiens* along Canonical Axis 1 (CAN1) (fig. S7A). The *Ar. ramidus* hand falls within the *Pan* distribution along CAN1 and Canonical Axis 3 (CAN3) (fig. S7B). Additional details on the coefficients of linear discriminants (table S5) can be found in the Supplementary Materials.

We examined multivariate variation in MCP and interphalangeal (IP) joint shape using PCA on six logged geometric mean-standardized measurements [MC5 head mediolateral breadth (MC5 HML); MC5 head dorsopalmar depth (MC5 HDP); PP3 trochlea mediolateral breadth (PP3 TML); PP3 trochlea dorsopalmar depth (PP3 TDP); IP3 trochlea mediolateral breadth (IP3 TML); IP3 trochlea dorsopalmar depth (IP3 TDP)] that are linked to the mechanics of suspension (Fig. 2A). In unimanual suspension with the hand positioned in a “hook grip” on a circular horizontal support (9, 31) and with the MCP joint in approximately 90° of flexion (32), the force of body weight (mg) creates an extension moment at the MCP joint with an external moment arm (R) determined by the distance between the weight vector and the support reaction force (SRF). Opposing MCP flexion moments are generated by the isometric force production (F_{FD}) of digital flexors (e.g., m. flexor digitorum profundus and m. flexor digitorum superficialis) and lumbricals with a moment arm length (r) influenced by the sagittal shape profile of the MCP joint (Fig. 2A). This simplified biomechanical model builds on previously published models describing the application of internal and external forces hypothesized to produce phalangeal stress and strain (32, 33). The points of application, positions, spatial orientations,

and magnitudes of external and internal force vectors, as well as the moment arm lengths, are hypothetical. Their purpose is to illustrate the biomechanical relevance of variation in MCP and IP joint shape in suspension.

The first PC accounts for 62% of the variance, and positive values are associated with decreased MC5 HML, increased PP3 TDP, and increased IP3 TDP (Fig. 2B). Higher values of PC1 therefore reflect increases in morphological measurements hypothetically correlated with the moment arms of the extrinsic digital flexors (e.g., m. flexor digitorum superficialis and m. flexor digitorum profundus). Hylobatids, *Pan*, *Pongo*, *Gorilla*, and atelines (*Ateles*, *Brachyteles*, and *Lagothrix*) fall to the right of papionins, cercopithecins, and colobines along PC1, with some overlap between gorillas and arboreal cercopithecoids and platyrrhines (Fig. 2B). *Ar. ramidus* falls within the ranges of variation of *Pan troglodytes*, *Gorilla gorilla*, and *Pongo* and above the ranges of variation of all cercopithecoids and platyrrhines. *Australopithecus* and *Homo* fall within the range of variation of *H. sapiens*, which occupies the negative end of PC1 overlapping with arboreal cercopithecoids and platyrrhines. The *Ar. ramidus* ARA-VP-6/500 hand does not preserve the head of the third metacarpal (MC3), so we necessarily analyzed the articular dimensions of the preserved MC5 head alongside the PP3 and IP3 dimensions. Our biomechanical model depicts the MCP and interphalangeal joints of the third ray (i.e., including the third metacarpal head), but it applies to all nonpollical rays.

We examined MC1 traits hypothesized to reflect the ability of modern humans and fossil hominins to generate forceful pollical grips and to reduce stress at the pollical MCP and carpometacarpal joints [i.e., MC1 head breadth, MC1 head depth, MC1 cross-sectional area (product of MC1 MSML and MC1 MSDP), and MC1 base area (product of MC1 BML and MC1 BDP)] associated with stone tool-related behaviors (30, 34). Modern humans have dorsopalmarly deeper (fig. S8A), mediolaterally wider (fig. S8B) MC1 heads combined with large diaphyseal cross-sectional and base areas relative to overall hand size (quantified as the geometric mean of 26 metrics) compared to other taxa (fig. S8, C and D). *H. neanderthalensis*, *H. naledi*, *Au. sediba*, and *Au. afarensis* tend to be most similar to modern humans in most of the comparisons, whereas *Ar. ramidus* is consistently *Pan*-like. However, *H. naledi* has an exceptionally small MC1 base relative to hand size, as initially noted by Kivell and colleagues (35), and is similar to *Ar. ramidus* and *Pan* (fig. S8C). In addition, *Au. sediba* has an MC1 base area that is intermediate between *Homo* and *Pan* relative to hand size.

Phalangeal curvature

Phalangeal curvature reduces diaphyseal strain associated with suspension (32, 33) and is therefore an important correlate of primate positional behavior (19, 30, 36, 37). To clarify how phalangeal curvature in the *Ar. ramidus* hand compares to our comparative sample, we quantified the curvature of the PP3 in a large sample of anthropoids and fossil taxa using the included angle method (Fig. 3). The overall pattern of phalangeal curvature in the extant and fossil sample is consistent with that of previous studies (19, 36, 37). The phalanges of *Hispanopithecus*, *Danuvius*, and *Ar. ramidus* are characterized by pronounced curvature, falling within the ranges of variation of the most suspensory anthropoids (*Pan*, *Pongo*, hylobatids, and atelines; Fig. 3). The phalanges of the remaining Miocene hominoid taxa (*Pierolapithecus*, *Griphopithecus*, *Ekembo*, *Sivapithecus*, and *Oreopithecus*) as well as *Au. afarensis* and *Au. sediba* fall within the

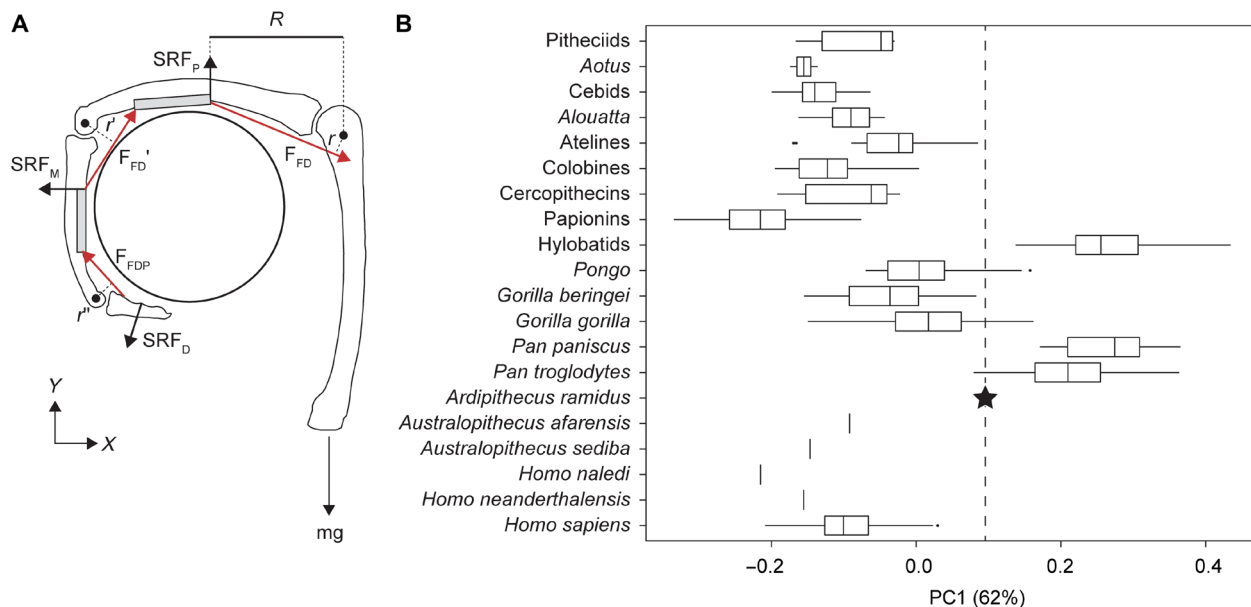


Fig. 2. MCP and interphalangeal joint shape contributes to suspensory performance. (A) Free-body diagram depicting the third ray of a siamang positioned in a hook grip on a horizontal support following (32). The points of application, spatial orientations, and magnitudes of external and internal force vectors, as well as moment arm lengths, are hypothetical. Joint reaction forces are not depicted here for the sake of clarity. SRF, support reaction force (near proximal, middle, and distal phalanges); R , external moment arm; r , internal moment arm; F_{FD} , muscle force vector associated with the flexor digitorum muscles (m. flexor digitorum superficialis and m. flexor digitorum profundus); $F_{FD'}$, muscle force vector associated with the m. flexor digitorum profundus. Flexor forces applied to the support are the vertical components of F_{FD} and F_{FDP} and the horizontal component of $F_{FD'}$. (B) Major axis of variance derived from a PCA on six logged geometric mean-standardized measurements (MC5 HML, MC5 HDP, PP3 TML, PP3 TDP, IP3 TML, and IP3 TDP). Positive values of PC1 are associated with decreased MC5 head breadth, increased PP3 TDP, and increased IP3 TDP.

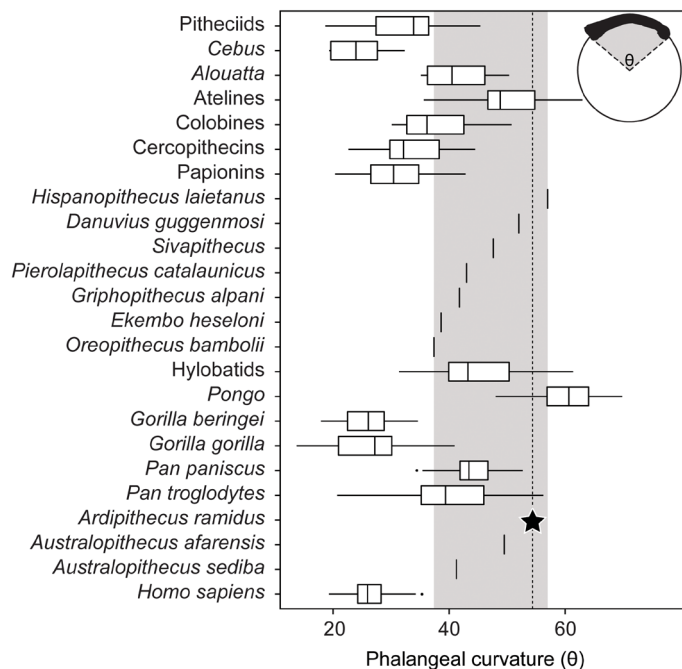


Fig. 3. Proximal phalangeal curvature in anthropoid primates. The gray bar indicates the range of variation among the Miocene fossil hominoids included here. The curvature of the *Ar. ramidus* PP3 falls within the ranges of variation of *P. troglodytes*, *Pongo*, hylobatids, and atelines; between the highly suspensory Miocene hominoids *Danuvius* and *Hispanopithecus*; and above the ranges of variation of all other taxa.

overlapping ranges of multiple anthropoid taxa including *Pan*, hylobatids, cercopithecins, and colobines.

Evolutionary modeling

To test alternative hypotheses about the relationship between hand morphology and locomotor behavior, we reconstructed the adaptive landscape of primate hand evolution using phylogenetic comparative methods [(38, 39); see also (5, 22, 40)]. These methods allow us to translate adaptive hypotheses into explicit evolutionary models tested against comparative data in a maximum likelihood framework. They also allow us to estimate evolutionary parameters such as the optimal hand morphology for a given selective regime (i.e., locomotor category).

Our evolutionary modeling analyses use the first three PCs from our PCA to reduce the dimensionality of the dataset. In our a priori adaptive hypotheses (fig. S9), we assigned *Australopithecus* and *Homo* to their own selective regime and *Ar. ramidus* to the same regime as *Pan* given the results of our morphometric analyses. The first hypothesis (H_1) recognizes taxa that are mostly terrestrial (*Gorilla beringei*, *Papio*, *Theropithecus*, and *Mandrillus*), those that are semiterrestrial (*Pan*, *G. gorilla*, *Semnopithecus entellus*, *Macaca mulatta*, *Macaca nemestrina*, *Macaca nigra*, *Cercocebus*, and *Chlorocebus aethiops*), those that are mostly arboreal (all other non-hominin taxa), and those who frequently use their hands in nonlocomotor contexts including *Homo* and *Australopithecus*. The second hypothesis (H_2) is identical to H_1 but separates mostly arboreal quadrupedal taxa from those that are more suspensory (*Pongo*, hylobatids, *Ateles*, and *Brachyteles*). The third hypothesis (H_3) includes regimes for digitigrade taxa (*M. mulatta*, *M. nigra*, *Papio*, *Theropithecus*, *Mandrillus*, and *Cercocebus*), knuckle-walking

taxa (*Pan* and *Gorilla*), suspensory taxa (*Pongo*, hylobatids, *Ateles*, and *Brachyteles*), nonlocomotor taxa (*Homo* and *Australopithecus*), and palmigrade taxa (all remaining anthropoids). We tested an alternative hypothesis (H_4) based on H_3 in which we placed *Pan* and *Ardipithecus* in a regime with the suspensory taxa and *Gorilla* in its own terrestrial knuckle-walking regime (fig. S9). The assignment of cercopithecoid taxa into locomotor or hand posture categories was based on published literature (41). Next, we used SURFACE to identify selective regimes based on morphological similarity without identifying them a priori (39), which has been used previously to test hypotheses of human and primate evolution (5, 22, 40). Last, we tested the relative support of our results with two simpler alternative evolutionary hypotheses including evolution by genetic drift (i.e., Brownian motion; H_{BM}) and adaptation with a single optimum [i.e., Ornstein-Uhlenbeck (OU); H_{OU1}]. Support for H_{BM} or H_{OU1} would suggest that our data do not reflect an adaptive signal related to locomotor behavior.

Our results show that hand morphology is best described by 11 selective regimes with all a priori adaptive hypotheses performing worse than the SURFACE model (Fig. 4 and tables S6 and S7). The selective regimes identified by SURFACE likely reflect a combination of locomotion and other factors (Fig. 4 and table S7). For example, the best supported a priori model fit using the “ouch” package in R included a convergent suspensory regime containing atelines and Asian hominoids, but SURFACE separated them into distinct regimes that likely reflect their distinct evolutionary histories (e.g., *Ateles* and *Brachyteles* pollical reduction) and body sizes. Likewise, we found support for terrestrial knuckle-walking (*Pan* and *Gorilla*) and digitigrady (*M. mulatta*, *M. nigra*, *Papio*, *Theropithecus*, *Mandrillus*, and *Cercocebus*) regimes that were subsequently separated by SURFACE. Note that SURFACE identified three regimes representing the spectrum of nonsuspensory quadrupedal hand postures and substrate preferences among cercopithecoids and platyrrhines ranging from arboreal palmigrady to terrestrial digitigrady, mostly reflecting variation in metacarpal and phalangeal lengths relative to the hand geometric mean. *Colobus* was placed in its own regime nearest the arboreal palmigrady optimum reflecting evolution in the direction of the *Ateles* and *Brachyteles* regime associated with pollical reduction. SURFACE placed *Ar. ramidus* into a regime with *Pan paniscus* and *P. troglodytes*, suggesting adaptation to an optimal hand shape related to shared aspects of positional behavior, body size, and evolutionary history. SURFACE detected an evolutionary shift in hand morphology between the *Homo-Pan* ancestral phenotypic optimum, including *Ardipithecus* and *Pan*, and all later hominins primarily related to decreased intrinsic phalangeal length and increased MC1 length.

In addition to testing adaptive hypotheses, the OU model allows for the estimation of evolutionary parameters such as the phylogenetic half-life ($t_{1/2}$; table S7), which is the average time it takes to evolve half the distance from the ancestral optimum to a new optimum given a regime shift. The phylogenetic half-life ($t_{1/2}$) therefore quantifies the rate of adaptation. The estimate of $t_{1/2}$ for PC1, which is the axis separating the ancestral hominin optimum from the primary hominin optimum, is 722 ka (thousand years) (table S7), which is relatively fast evolution compared to the total length of the tree [46.8 Ma (million years)]. As discussed above, PC1 is primarily associated with the intrinsic lengths of the metacarpals and phalanges. The estimates of $t_{1/2}$ for PC2 and PC3 are 1.26 Ma and 5 ka, respectively. PC2 and PC3 are associated with metacarpal

length, joint, and midshaft dimensions. The estimates of the phylogenetic half-life for each PC suggest that anthropoid metacarpal length and midshaft dimensions (i.e., MC1 relative to MC5) have evolved more slowly than phalangeal lengths and articular dimensions (e.g., the ulnar carpometacarpal and MCP joints). We used a Monte Carlo simulation method (42) to evaluate the statistical power to distinguish between alternative evolutionary models given our dataset and phylogeny (fig. S10). The simulation results show that all models can be distinguished from each other and support information criteria metrics [Akaike information criterion (AIC), small sample size corrected Akaike information criterion (AICc), and Schwarz information criterion (SIC)]. Previous studies have criticized the use of SURFACE for multivariate evolutionary modeling (43). We include the use of SURFACE for explicit comparison to recent similar studies (5, 22, 40) and as an additional perspective to our a priori models fit using the ouch package (38) in R. Overall, our use of Monte Carlo simulations provides additional support for the model fit by SURFACE.

We conducted a SURFACE analysis using the first three PC scores derived from our PCA on a modified dataset including *H. laietanus* (fig. S11 and table S8). SURFACE identified nine select regimes including a convergent regime containing *H. laietanus*, *Pongo*, *Lagothrix*, and *Ateles*. The locations of the evolutionary shifts estimated by SURFACE resemble our initial analysis using a larger dataset but with some differences. *Ar. ramidus* is placed in the same selective regime with *P. troglodytes* and *P. paniscus*, but expectedly, the analysis on the reduced dataset also places *Au. afarensis* in this regime since it excludes MC1 data. The *Au. afarensis* hand clusters with *Au. sediba*, *H. naledi*, and *H. neanderthalensis* in the PCA (fig. S5) but is distinguished from them along PC3 (fig. S11), which is associated with MCP and IP joint dimensions and MC4 length (table S2). Instead, SURFACE detects an evolutionary shift at the base of the *Au. sediba* and *Homo* clade. In addition, colobines, cercopithecins, and most papionins are placed in a single regime with evolutionary shifts toward a more terrestrial digitigrady regime in *Papio* and *Theropithecus*. Overall, the results of our SURFACE analysis on a modified dataset are consistent with our initial analyses because it recovers an evolutionary shift at the base of the great ape clade associated with suspensory adaptations.

Ancestral estimations of human and great ape hand morphology

We estimated the ancestral hand morphology for humans and great apes using StableTraits software (44). StableTraits uses a stable model of continuous trait evolution to estimate ancestral values without assuming neutrality and gradualism, which accommodates a more biologically plausible set of evolutionary processes that produce evolutionary rate heterogeneity across the phylogeny. A Markov chain Monte Carlo (MCMC) algorithm was used to estimate the posterior distributions of ancestral states for each internal node of the phylogeny. We performed separate ancestral estimations on the first three PCs derived from our PCAs on our full (fig. S1) and modified datasets (fig. S5), which we visualized as phylomorphospace plots constructed using the “phytools” package (45) in R (Fig. 5). The hand morphology of the *Homo-Pan* LCA is estimated to be more similar to *Pan* than to any other extant taxon sampled here (Fig. 5, A and B). The 95% credible interval on the estimated hand morphology of the *Homo-Pan* LCA using our 26-variable dataset includes the mean value of *G. gorilla* along PC1 and PC3 and the

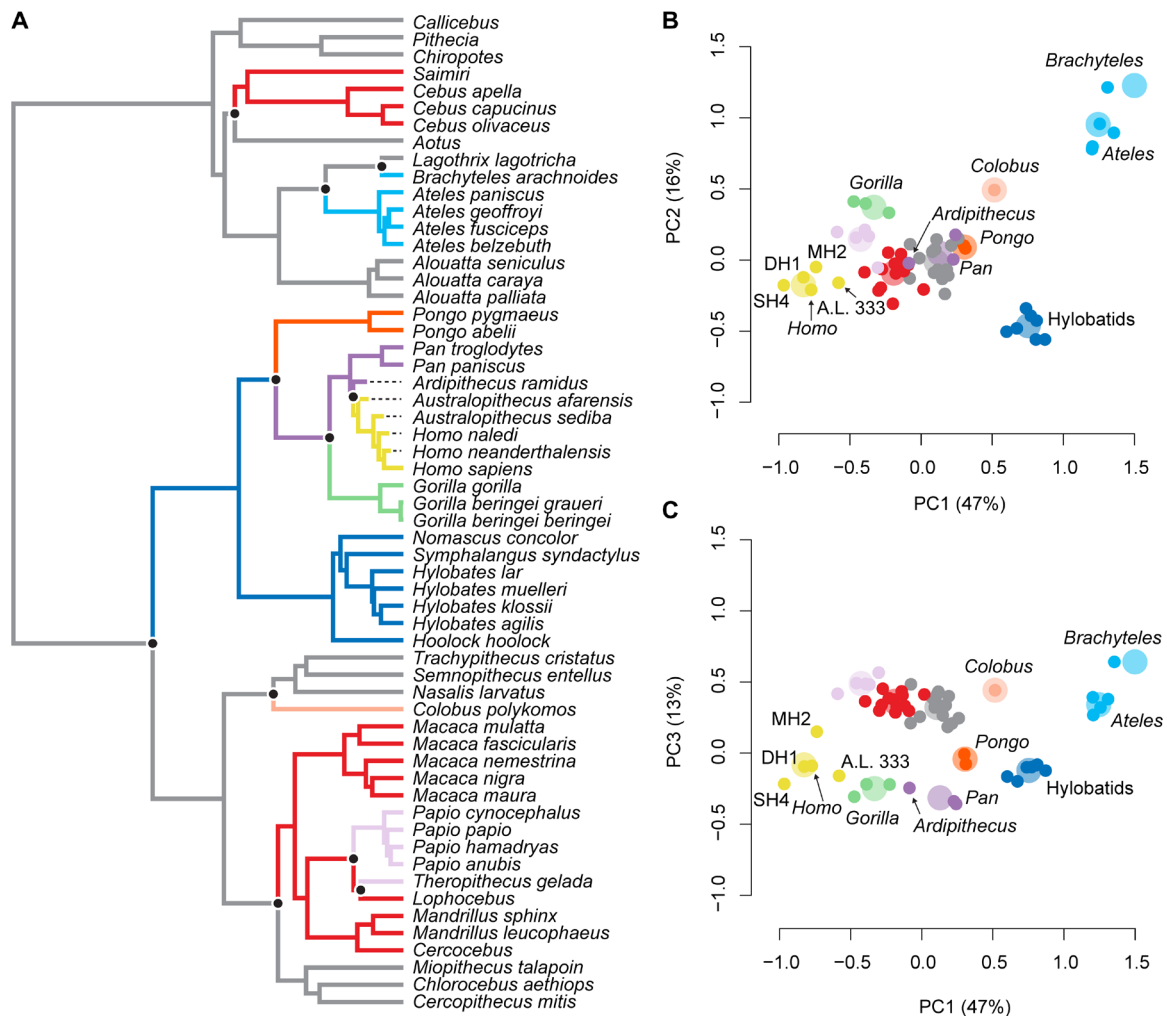


Fig. 4. The evolution of anthropoid hand shape according to SURFACE. (A) Phylogenetic tree with branches painted according to selective regime. **(B)** Species means for PC1 and PC2 (small circles) and estimated phenotypic optima (large circles). **(C)** Species means for PC1 and PC3 (small circles) and estimated phenotypic optima (large circles). *Ar. ramidus* was placed in the same selective regime as *P. troglodytes* and *P. paniscus*. In contrast, all later hominins were placed in a selective regime with modern humans, which results in an evolutionary shift in hominin hand morphology from a *Pan*-like ancestor between ca. 4.4 and 3.2 Ma ago.

mean value of *P. paniscus* along PC2. The 95% credible interval on the estimated hand morphology of the *Homo-Pan* LCA using our 17-variable dataset includes the mean value for *P. troglodytes* along the first three PCs.

The results of our evolutionary modeling and ancestral estimation analyses provide complementary perspectives on the evolution of ape and human hands. For example, our initial SURFACE analysis estimated a large morphometric discontinuity between the estimated phenotypic optima for palmigrade monkeys and suspensory apes (Fig. 4). The 95% credible intervals for the ancestral hand morphology of great apes occupy this area of the morphospace between extant palmigrade monkeys and suspensory apes, consistent with ape evolution from an arboreal palmigrade ancestor (Fig. 5, C and D). Along the first two PCs, the estimated ancestral hand morphology of great apes includes *H. laietanus*, *P. paniscus*, *Pongo*, and *Lagothrix*. Overall, our ancestral estimations and evolutionary modeling analyses are consistent with the presence of suspensory adaptations in the hands of the LCA of great apes (18).

Relative size and scaling of metacarpal and phalangeal lengths

Last, we used phylogenetic generalized least squares (*p*GLS) to estimate the regression of log metacarpal and phalangeal lengths on log body mass using the “caper” package in R (Fig. 6 and table S9) (46). *Ardipithecus*, *Pierolapithecus*, *Hispanopithecus*, and *Danuvius* were excluded from the models, but plotted with the other data, given the uncertainties of their body mass estimates and the phylogenetic positions of the Miocene hominoids. Length of the MC1 relative to body mass shows substantial overlap between taxa and variation within locomotor modes. For example, *H. sapiens*, *H. neanderthalensis*, and *H. naledi* do not have relatively longer MC1s than *Pan*. Among the suspensory taxa, hylobatids have the longest MC1s and *Ateles* the shortest. *Ardipithecus* is similar to *Homo* and *Pan* in the relative length of the MC1 (Fig. 6A). *Australopithecus* and *Homo* have the relatively shortest MC5 lengths, which contributes to their high thumb-to-digit ratio (13, 15, 22). Terrestrial monkeys overlap with the more suspensory taxa (hylobatids, *Ateles*, and *Pongo*) and *Pan*

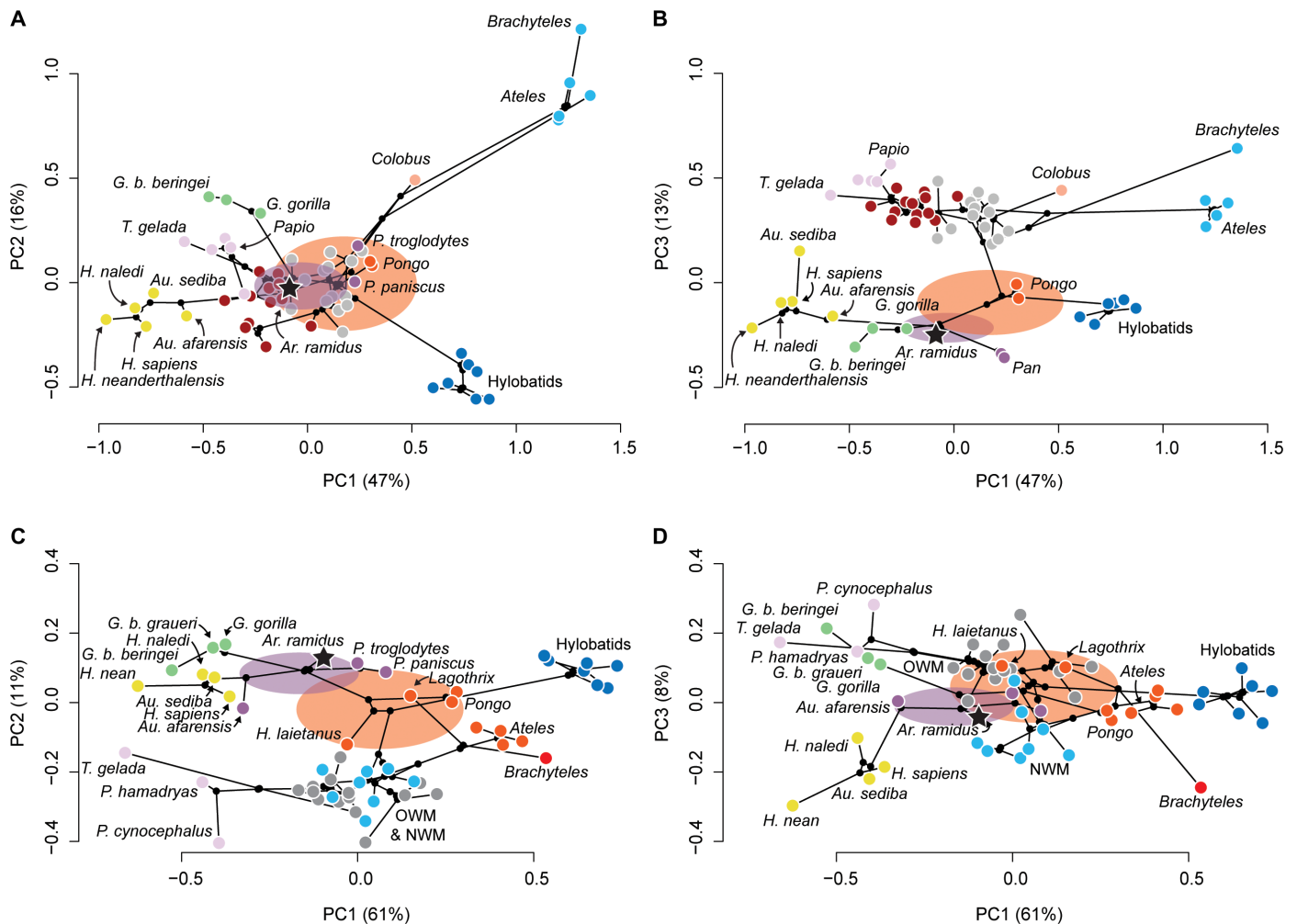


Fig. 5. Phylomorphospace plots and ancestral estimations. (A) PC1 and PC2 computed from PCA on 26 variables. (B) PC1 and PC3 computed from PCA on 26 variables. (C) PC1 and PC2 computed from PCA on 17 variables including *H. laietanus*. (D) PC1 and PC3 computed from PCA on 17 variables including *H. laietanus*. Purple ellipses, 95% credible intervals for the ancestral hand morphology of humans and chimpanzees. Orange ellipses, 95% credible intervals for the ancestral hand morphology of great apes. Points represent species means, except in the case of fossils, and their colors correspond to selective regimes identified by SURFACE for each dataset. OWM, Old World monkey; NWM, New World monkey.

in the relative length of the MC5. *Ar. ramidus* is intermediate between *Pan* and *Gorilla* in the relative length of the MC5 (Fig. 6B). The most suspensory taxa have relatively long phalanges of the third digit, whereas small-bodied arboreal quadrupeds, terrestrial monkeys, and other fossil hominins tend to have the relatively shortest phalanges (Fig. 6C). *Nasalis* has the largest body mass and the relatively longest phalanges of the arboreal cercopithecoids sampled here. *Ar. ramidus* is most closely aligned with *P. paniscus* and *Danuvius*, and intermediate between *Hispanopithecus* and *Pierolapithecus*, in the relative lengths of the third digit phalanges (Fig. 6D).

DISCUSSION

Our results show that, despite subtle differences from modern suspensory apes (e.g., decreased MC5 length), the *Ar. ramidus* hand (ARA-VP-6/500) displays morphometric affinities with great apes and shared a selective regime with modern chimpanzees and bonobos.

First, morphometric analyses of the preserved metacarpals and phalanges of the ARA-VP-6/500 hand show that PCA separates extant anthropoid primates according to known differences in hand morphology that are related to behavioral differences (Fig. 1 and fig. S1), and *Ardipithecus* is most similar to extant great apes (Figs. 1 to 5). Building on this result, we found that both *Ar. ramidus* and *Au. afarensis* fall along a hypothetical evolutionary trajectory from a more chimpanzee-like, rather than monkey-like, LCA (Fig. 1). Second, we found that the relative length and curvature of the PP3 of *Ar. ramidus*, along with the shape of the MCP and proximal interphalangeal (PIP) joints, are most closely aligned with suspensory apes (Figs. 2 and 3). Last, we reconstructed the macroevolutionary adaptive landscape for the anthropoid hand and found that *Ar. ramidus* likely shared primitive suspensory adaptations with modern chimpanzees and bonobos, before an evolutionary shift detected at the base of the *Australopithecus* and *Homo* clade (Fig. 4). Hominin hand evolution from a more suspensory, ape-like ancestor rather

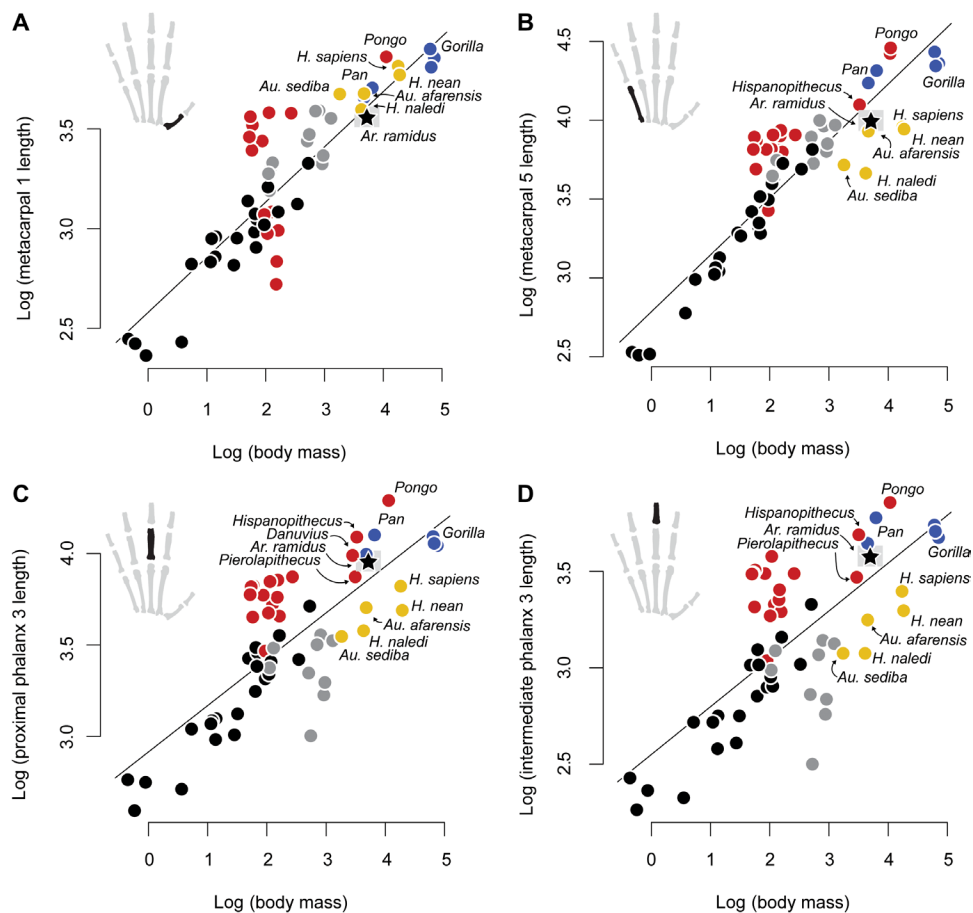


Fig. 6. pGLS regression between manual ray segment lengths and body mass in anthropoid primates. (A) Relationship between MC1 length and body mass. (B) Relationship between MC5 length and body mass. The MC5 length of *Hispanopithecus* was estimated from its MC4 length using regression. (C) Relationship between PP3 length and body mass. (D) Relationship between IP3 length and body mass. Black symbols, palmigrady; gray symbols, digitigrady; red symbols, suspensory; blue symbols, knuckle walking; gold symbols, nonlocomotor (manipulative). The gray box surrounding *Ar. ramidus* represents the range of body mass estimates.

than a more generalized, monkey-like ancestor is also supported by ancestral estimations (Fig. 5). Collectively, these results falsify the hypothesis that hominins evolved from an ancestor with a generalized hand that lacked suspensory adaptations (2–4, 10–12, 22).

The results of our evolutionary analyses contradict the original suggestion that the hand of *Ar. ramidus* is Old World monkey-like in intrinsic proportions (2, 3) or generalized relative to extant hominoids (22), which can be explained through both analytical and methodological differences. Our PC1 mostly reflects hand length and shares similarities to the one presented in a recent study including the *Ar. ramidus* hand (22). Critically, this multivariate axis alone cannot distinguish between African ape-like and monkey-like hypotheses for the hand of the LCA. The position of *Ar. ramidus* between *Pan* and *Homo* along PC1 (and within the “monkey” range of variation) is consistent with both hypotheses. Either *Ar. ramidus* had evolved away from an African ape-like LCA or, alternatively, retained an ancestral monkey-like hand. Our inclusion of more data (i.e., articular and midshaft dimensions) and increased taxonomic breadth results in better separation on subsequent PCs (i.e., variance is distributed among more PCs) and shows that a generalized, monkey-like hand for the *Homo-Pan* LCA is not supported by the fossil and comparative data.

Hand morphology and positional behavior

We interpret the shared aspects of nonpollical metacarpal and phalangeal morphology of *Ar. ramidus*, *Pan*, and, by estimation, the *Homo-Pan* LCA to reflect the use of below-branch, suspensory posture and locomotion as part of a varied positional repertoire including arboreality, vertical climbing, and, among the latter two, terrestrial quadrupedalism. The relatively long and curved phalanges of *Ar. ramidus* allowed for the application of a greater proportion of its digital flexor force to horizontal supports in below-branch suspension while reducing diaphyseal strain (32, 33). The proportion of the flexor force applied to the support contributes to the force of static friction (e.g., equivalent to the sum of the vertical components of F_{FD} and F_{DP} and the horizontal component of F_{FD}' in Fig. 2A multiplied by the coefficient of friction), which opposes motion between the digits and the support (33, 47).

The MCP and PIP joint morphology of *Ar. ramidus* is characteristic of a digital joint complex hypothesized to increase the magnitude of internal flexion moments produced by the extrinsic digital flexors, which is an important feature of below-branch positional behavior. Previous studies have noted the “flexion set” of metacarpal heads (9, 48) and phalangeal trochleae (49), as well as the relatively tall MCP and PIP joints of extant hominoids (20, 49), which

would act to increase the moment arms of the long digital flexors, particularly in more flexed positions. In addition, the larger moment arms of hominoid digital flexors are associated with relatively large flexor musculature, implying increased ability to generate large moments at the MCP and PIP joints (50, 51). The characteristics of the forelimb musculature of *Ar. ramidus* are unknown, but the projections of its scaphoid tuberosity and hamate hamulus are consistent with a deepening of the carpal tunnel (2). Accordingly, the MCP and PIP joint morphology of *Ar. ramidus* is more closely aligned with *Pan* and *Pongo* than more generalized arboreal quadrupeds (Fig. 2B), implying a greater ability to generate forceful MCP joint flexion, which provides evidence for adaptation to suspensory locomotion in early hominins and the *Homo-Pan* LCA.

The relative length of the *Ar. ramidus* MC5 is intermediate between *Pan* and *Gorilla* but greater than that of all other hominins. Metacarpal length has mechanical consequences in the context of varied positional repertoires, hand postures, and substrate preferences. Nonpollical metacarpal length has been argued to be a correlate of suspensory positional behaviors (2, 21). The presence of shorter metacarpals relative to support diameters may cause increases in wrist flexion during suspension (31). However, metacarpal length increases do not positively contribute to performance in suspensory postures (e.g., uni- or bimanual arm hanging) and may only partly contribute to performance in forms of suspensory locomotion (e.g., brachiation and bridging) as a constituent of upper limb length. In brachiation,

bridging, and vertical climbing, a longer upper limb allows individuals to travel greater distances per stride, which is hypothesized to reduce both metabolic energy expenditure and the probability of deficient grasps that could lead to deadly falls (33). The reconstructed upper limb length of *Ar. ramidus* suggests that it was not adapted to hylobatid-like, ricochet brachiation or *Pongo*-like quadrumanous climbing and bridging (2). Instead, the hand of *Ar. ramidus* and the estimated morphology of the *Homo-Pan* LCA are more consistent with a *Pan*-like positional repertoire including orthograde vertical climbing and suspension. Therefore, it is premature to reject hypotheses of adaptation to below-branch suspension among fossil hominoids and early hominins on the basis of metacarpal length alone given its functional role in various primate positional repertoires, substrate preferences, and hand postures (33, 36, 41, 52).

A recent multivariate analysis of foot proportions suggested that the positional repertoire of *Ar. ramidus* and the *Homo-Pan* LCA also included terrestrial heel-strike plantigrady and vertical climbing (5). The presence of a suspensory adapted hand and a terrestrially adapted foot in *Ar. ramidus* and the *Homo-Pan* LCA is notable because this combination is only observed among extant knuckle-walking apes. The knuckle-walking hand posture is a compromise that enables large-bodied suspensory apes to spend a significant proportion of their time on the ground (51). Functionally, knuckle walking reduces external moments at the MCP joints despite the retention of

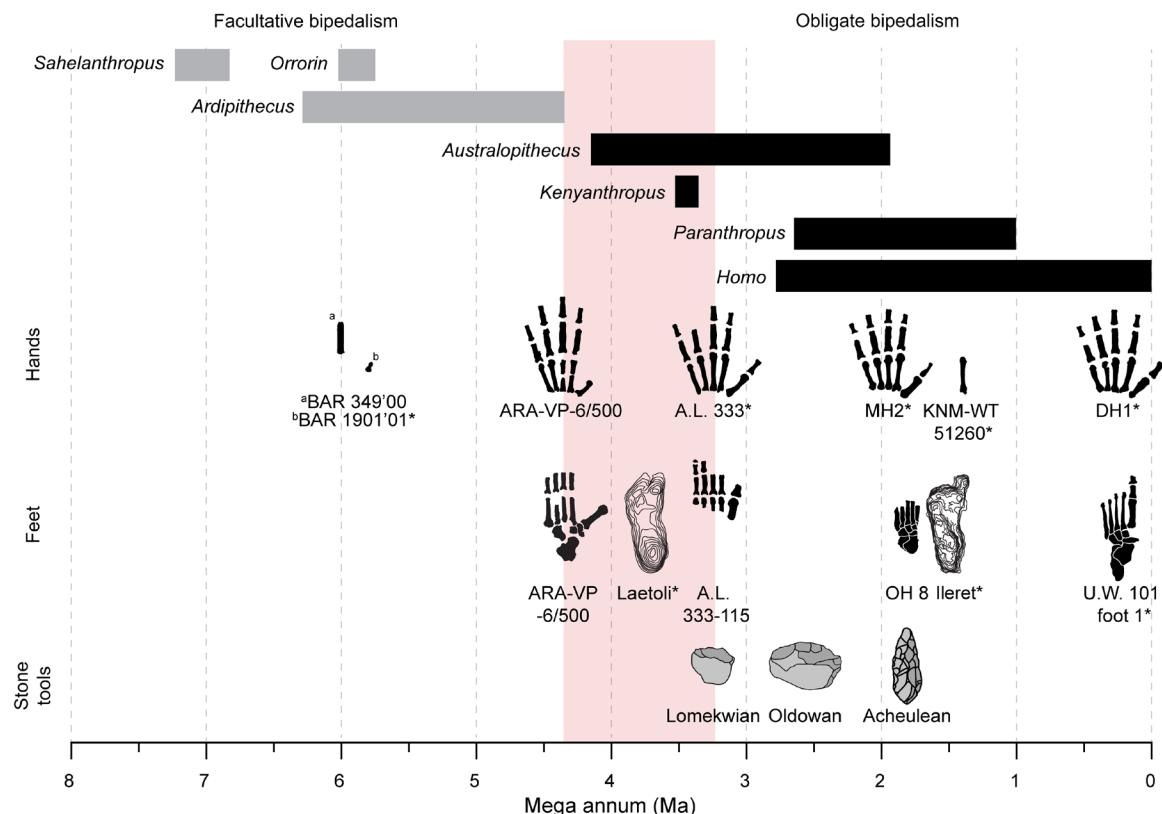


Fig. 7. The evolution of hominin hands and feet reflects an evolutionary shift toward enhanced manipulative capabilities and obligate bipedalism, respectively. Partial hands, partial feet, and stone tool exemplars are depicted here and supplemented by reference to more fragmentary specimens preserving functionally relevant anatomies. Gray bars, facultative bipedalism; black bars, obligate bipedalism; red bar, approximate timing of hypothesized hominin evolutionary shift. Asterisks indicate that the fossil was mirrored. BAR 349'00, curved juvenile manual proximal phalanx of *Orrorin tugenensis*; BAR 1901'01, pollical distal phalanx of *O. tugenensis* with extrinsic flexor insertion; OH 8, foot attributed to *Homo habilis*; KNM-WT 51260, MC3 with styloid process probably representing *Homo erectus*; U.W. 101 (foot 1), partial foot of *H. naledi*.

elongated phalanges (36). The suspensory hand of *Ar. ramidus*, its terrestrial plantigrade foot posture (5), and the retention of knuckle-walking features in the wrists of early hominins (1), as well as other African ape-like regions of the skeleton (53–55), provide indirect support for the knuckle-walking hypothesis. Our evolutionary modeling analyses and ancestral estimations strongly support a more *Pan*-like, rather than monkey-like, hand morphology for the *Homo-Pan* LCA, which raises the critical question of which hand posture the LCA would have used if it was not a knuckle walker. We interpret the evolution of African ape knuckle walking to be contingent upon evolution from an ancestor adapted to climbing and suspension (51). Therefore, suspension, vertical climbing, and knuckle walking are naturally linked from both functional and evolutionary perspectives. Ultimately, the definitive resolution of the knuckle-walking hypothesis relies on the recovery of direct fossil evidence of chimpanzee and gorilla postcranial evolutionary history, but we interpret the preponderance of the available fossil and comparative evidence to support hypotheses of a large-bodied, semiterrestrial, knuckle-walking LCA with adaptations to climbing, suspension, and heel-strike plantigrady (1, 5, 40, 53–55, 81).

Hominin hand morphology, manipulative behavior, and bipedalism

We identified an evolutionary shift between *Ar. ramidus* and all later hominins that has been subsequently maintained for 3 Ma or more despite the gradual evolution of refinements to the hand and wrist throughout the Plio-Pleistocene (30, 34, 56–58). This evolutionary shift occurs within temporal proximity of the earliest known stone tools at Lomekwi 3, Kenya dated to 3.3 to 3.5 Ma (59) and stone tool cut marks on bones from Dikika, Ethiopia dated to >3.39 Ma (60). The evolutionary shift in hominin hand morphology implies a major difference between *Ar. ramidus* and later hominins in manipulative performance capabilities (34). The morphology and anatomy of chimpanzee and bonobo hands do not impede their use of organic tools in the wild, including the occasional use of unmodified stones by some chimpanzee populations, but they lack the intrinsic hand proportions, joint dimensions, and hypertrophied thenar and hypothenar musculature required to generate the forceful precision grips characteristic of hard hammer percussion (34, 56, 61–64). The hand of *Ar. ramidus* also lacks many of these important functional characteristics related to stone tool manufacture. The presence of tool-using behaviors among all extant great apes, combined with the ubiquitous use of more elaborate tools by chimpanzees, implies that the *Homo-Pan* LCA probably used tools (64, 65). Currently, there is no archeological evidence for hominin-like stone tool manufacture earlier than ca. 3.3 to 3.5 Ma, but we acknowledge that future discoveries may show otherwise. Nonetheless, with a synthesis of new evidence, we interpret the shared-derived aspects of *Australopithecus* and *Homo* hand morphology and the functional implications of their difference from *Ar. ramidus* to reflect adaptation to manipulative behaviors probably involving stone tool manufacture in some manner (Fig. 7).

Compared to *Ar. ramidus*, the shorter nonpollical metacarpals and phalanges of *Australopithecus* and *Homo* allow for the formation of forceful precision grips when combined with an intrinsically elongated first ray (22, 25, 30, 34, 56, 61). The intrinsically longer MC1 of *Australopithecus* and *Homo* compared to *Ar. ramidus*, *Pan*, and *Gorilla* increases the moment arms of the thenar muscles (34, 62), which enables them to generate large-magnitude internal moments

to oppose large-magnitude external moments generated by tool reaction forces hypothesized to be characteristic of hard hammer percussion (63). The increased dorsopalmar depth of the MC1 head relative to hand size in *Australopithecus* and *Homo* is consistent with the production of larger-magnitude internal moments at the pollical MCP joint (fig. S8A). Biomechanical modeling supports the hypothesis that human hand proportions enhance manual dexterity (66) and that the phenotypic optimum occupied by *Australopithecus* and *Homo* is consistent with enhanced manipulative performance (67).

At the same time, the *Au. afarensis* hand displays primitive retentions that may suggest some manipulative performance deficits relative to later hominins (56, 68, 69). The *Au. afarensis* MC5 (A.L. 333-14) has an ape-like palmar extension of its hamate facet, indicating articulation with the hook of the hamate, which is hypothesized to limit ulnar carpometacarpal flexion and supination useful for opposing the fifth digit with the pollex during manipulative behaviors (62, 69). Furthermore, the *Au. afarensis* MC1 (A.L. 333w-39) has a *Pan*-like origin of the first dorsal interosseous muscle (57), the trapezium (A.L. 333-80) has a strongly curved MC1 facet, and the MC3 (A.L. 333-16) lacks a styloid process (57, 58, 70). We acknowledge that the A.L. 333 hand sampled here is a composite of specimens potentially representing multiple individuals (25). A recent resampling analysis suggested that *Au. afarensis* might have had hand proportions slightly more *Gorilla*-like than previously thought (29). Our multivariate analyses show that the morphology of the *Au. afarensis* hand is most similar to *Au. sediba* and *Homo* but with some proximity to extant gorillas along PC1. Overall, the hand morphology of *Au. afarensis* is consistent with the ability to use human-like precision grips, but it might have limited its ability to make advanced stone tools (56).

A series of derived postcranial traits indicate that *Ar. ramidus* used an early form of facultative bipedality (3–5, 71–73). Primitive retentions in limb morphology, including a grasping hallux, signify the importance of arboreality in the positional repertoire of *Ar. ramidus* (3, 4) despite the presence of a terrestrial plantigrade quadrupedal ancestry shared by the hominine clade (5, 27). The loss of a grasping hallux that permitted the use of large-diameter arboreal supports occurs as early as ca. 3.7 Ma according to the morphology of the Laetoli footprints (74) and certainly by ca. 3.2 Ma as evidenced by the morphology of the *Au. afarensis* foot fossils from A.L. 333 (75). The ca. 3.4 Ma hominin partial foot from Burtele, Ethiopia (BRT-VP-2/73) was initially suggested to provide evidence for the retention of a more *Ardipithecus*-like grasping foot into the Pliocene (76). However, recent work has shown that the Burtele hominin foot had a hallux proximal phalanx with a dorsally canted base; a mediolaterally widened, mildly dorsally domed first metatarsal head; low diaphyseal torsion; and a derived, asymmetric proximal articular surface of the first metatarsal, implying reduced hallux grasping capabilities relative to *Ar. ramidus* and extant apes (77). The presence of these features show that the Burtele hominin had a more derived hallux relative to *Ar. ramidus* capable of increased metatarsophalangeal dorsiflexion in bipedalism. In contrast, the first metatarsal of *Ar. ramidus* from Aramis lacks these metatarsophalangeal and tarsometatarsal joint features characteristic of later hominins (73), including the Burtele hominin, and instead has an overall more *Gorilla*-like morphology (77).

The evolution of hominin hallux adduction occurs alongside numerous other postcranial traits of the trunk, pelvis, and lower limb, indicative of a more derived form of obligate bipedalism in

Au. afarensis compared to *Ar. ramidus* (3, 4). To our knowledge, these observations provide the first fossil evidence to support the hypothesis of a coevolutionary shift in hominin postcranial morphology related to obligate bipedalism and manipulative behaviors probably involving stone tools (Fig. 7) (23–25, 28). The evolutionary mechanisms underlying this coevolutionary shift are unclear, but our observations complement the hypothesis that hominin hand evolution could have occurred as a correlated response to selection on pedal phalanges in relation to bipedalism due to genetic and developmental integration (28). Therefore, both paleontological and neontological data support the hypothesis that hominin hands and feet evolved in a correlated fashion (28).

Overall, our analysis demonstrates that the hand morphology of *Ar. ramidus* is more closely aligned with chimpanzees and bonobos than generalized quadrupeds, which supports the hypothesis that hominins evolved from an ancestor with a positional repertoire including suspension, vertical climbing, and, possibly, knuckle walking (1, 5–7, 27, 55). The foot skeleton of *Ar. ramidus* also suggests that the positional repertoire of the LCA included terrestrial plantigrade quadrupedalism and vertical climbing (5), supporting previous studies based on primate comparative anatomy and biomechanics (26, 27). The poor temporal resolution and fragmentary nature of the early hominin fossil and archeological records limit our ability to disentangle causes and effects in a satisfying manner. However, the hand morphology of *Ar. ramidus* differs substantially from that of *Au. afarensis* and all later hominins, marking a significant transition in the paleobiology and evolutionary history of hominins related to obligate bipedality, enhanced manipulation, and stone tool use and manufacture (23, 24, 28). New fossil discoveries in critical times and places will continue to throw light on this aspect of human origins.

MATERIALS AND METHODS

Data on extant anthropoid hand bones were collected at the following institutions: American Museum of Natural History, U.S. National Museum of Natural History, Harvard Museum of Comparative Zoology, Royal Museum for Central Africa, Cleveland Museum of Natural History, Berkeley Museum of Vertebrate Zoology, and Human Evolutionary Research Center at the University of California, Berkeley (table S10). The extant comparative sample includes 416 individuals representing hominoids, cercopithecoids, and platyrrhines for a total of 53 extant taxa. The mean number of individuals per taxon is 7.8 (SD = 11.9). We also present analyses using a modified dataset for the inclusion of *H. laietanus* composed of 369 individuals and 45 taxa (table S11). Some taxa are well sampled (e.g., *H. sapiens* and *P. troglodytes*), whereas others are represented by one or a few individuals because of availability in museum collections. Data on *Ar. ramidus* (ARA-VP-6/500), *Au. afarensis* (A.L. 333 composite), *Au. sediba* (MH2), *H. neanderthalensis* (Shanidar 4), and *H. laietanus* (IPS18800) were culled from the literature (2, 18, 25, 30, 70, 78). The original hand fossils of *H. naledi* (U.W. 101) and *Au. sediba* (MH2) were studied at the Evolutionary Studies Institute, University of the Witwatersrand (30, 35). Fossil hominoid phalangeal curvature was measured using published photographs of *H. laietanus*, *Pierolapithecus catalaunicus*, *Oreopithecus bambolii*, *Griphopithecus alpani*, *Ekembo heseloni*, *Sivapithecus*, and *D. guggenmosi*.

We collected standard linear measurements on metacarpals (MC1, MC4, and MC5), proximal phalanx 3 (PP3), and intermediate phalanx 3

(IP3) using digital calipers: maximum length (L), mediolateral breadth (BML) and dorsopalmar depth of the base (BDP), midshaft (MSML and MSDP), and head/trochlea (HML, HDP, TML, and TDP) (21, 36). The phalanges of the third digit were identified on the basis of their interdigital size and shape characteristics (e.g., length, robusticity, torsion, and asymmetries). We quantified proximal phalangeal curvature using photographs of phalanges using the included angle method following Susman and colleagues (37). The ARA-VP-6/500 partial hand of *Ar. ramidus* preserves pollical and nonpollical metacarpals and phalanges. Our analysis of the *Ar. ramidus* hand is focused on the well-preserved elements of the first and third rays (ARA-VP-6/500-015, MC1; ARA-VP-6/500-030, PP3; ARA-VP-6/500-059, IP3), but the second, third, and fourth metacarpals of the ARA-VP-6/500 hand are incomplete, so we instead included the MC5 (ARA-VP-6/500-036, MC5). We repeated our analysis of the *Ar. ramidus* hand using the available measurements of the fourth metacarpal (ARA-VP-6/500-010), whose length was estimated using regression by Lovejoy and colleagues (2), where possible. Our analysis of morphometric affinities is centered on the best-preserved elements of the *Ar. ramidus* hand to minimize uncertainty surrounding estimates of individual metrics given the primacy of questions surrounding its morphometric affinities. We took two approaches to evaluating the morphometric affinities of the *Ar. ramidus* hand. First, we standardized each raw measurement by their combined geometric mean to create scale-free shape variables for analysis. In addition, we log-transformed these shape-free variables because of the skewed distributions often produced by ratios. Second, we evaluated the size and scaling of metacarpal, proximal phalanx, and IP length relative to body mass. Body mass data for extant primates and estimates for fossil taxa (*Au. afarensis*, 39.1 kg; *Au. sediba*, 25.8 kg; *H. naledi*, 37.4 kg; *H. neanderthalensis*, 72 kg; *H. laietanus*, 33.5 kg; *P. catalaunicus*, 32.5 kg; *D. guggenmosi*, 31 kg) were culled from the literature (20, 40, 79–83). The body mass estimates for the ARA-VP-6/500 partial skeleton vary substantially, so we included both small (32.1 kg) and large (50.8 kg) estimates, as in previous studies (22, 40).

Our phylogenetic analyses use a consensus phylogeny based on molecular data of extant anthropoid primates with branch lengths proportional to elapsed time (84). *Ar. ramidus* was added to the consensus phylogeny for hominins as a stem hominin (85, 86). We used a branch length of 1.4 Ma for *Ar. ramidus* in accordance with the first appearance datum of *Ardipithecus kadabba* at 5.8 Ma and a last appearance datum of 4.4 Ma associated with the ARA-VP-6/500 partial skeleton (87). All other fossil hominin branch lengths were set to 1 Ma, except for *H. neanderthalensis*, whose branch length was estimated using a molecular method (84).

PCA on 26 scale-free variables was used to reduce the dimensionality of the dataset for evaluating morphometric affinities of the *Ar. ramidus* hand and for use of PC scores in subsequent evolutionary modeling analyses to maximize statistical power (42). In addition, PCA on 17 scale-free variables was used in supplementary analyses to include *H. laietanus*. Evolutionary modeling methods were used to test hypotheses about the link between hand morphology and locomotor behavior among anthropoid primates (38, 39). First, we used the *ouch* package (38) in R (88) to evaluate the fit of alternative a priori multiple-optimum OU models given our PC score data and phylogeny with an information criteria approach (e.g., AIC and AICc). Second, we used the “SURFACE” package (39) to fit a model without identifying selective regimes a priori and

compared it to our best-fitting a priori OU model using `ouch`. Last, we carried out Monte Carlo simulations to evaluate model fit as an alternative to information criteria (42).

We conducted ancestral estimations on PC scores derived from our PCAs on our full dataset of 26 variables and our reduced dataset of 17 variables using `StableTraits` software version 1.5 (44). Ancestral states were estimated using a constant-rate Brownian motion model and a stable model. In both analyses, we ran two independent Markov chains with 10,000,000 iterations at a thinning rate of 200, which resulted in 50,000 samples each. To prevent evolutionary rates from approaching zero, we used default priors on the evolutionary rate in `StableTraits`. The convergence of our two chains was assessed by evaluation of the proportional scale reduction factor value, which hovered ~ 1 (89). The first half of the iterations was discarded as burn-in. The Bayesian predictive information criterion provided support for the stable model over the constant-rate Brownian motion model (90). The ancestral state estimations and 95% credible intervals for the ancestral hominid and hominid nodes were visualized using a phylomorphospace plot constructed with the `phytools` package (45) in R (88).

SUPPLEMENTARY MATERIALS

Supplementary material for this article is available at <http://advances.sciencemag.org/cgi/content/full/7/9/eabf2474/DC1>

[View/request a protocol for this paper from Bio-protocol.](#)

REFERENCES AND NOTES

- B. G. Richmond, Evidence that humans evolved from a knuckle-walking ancestor. *Nature* **404**, 382–385 (2000).
- C. O. Lovejoy, S. W. Simpson, T. D. White, B. Asfaw, G. Suwa, Careful climbing in the Miocene: The forelimbs of *Ardipithecus ramidus* and humans are primitive. *Science* **326**, 70e1–70e8 (2009).
- C. O. Lovejoy, G. Suwa, S. W. Simpson, J. H. Matternes, T. D. White, The great divides: *Ardipithecus ramidus* reveals the postcrania of our last common ancestors with African apes. *Science* **326**, 100–106 (2009).
- T. D. White, C. O. Lovejoy, B. Asfaw, J. P. Carlson, Neither chimpanzee nor human, *Ardipithecus* reveals the surprising ancestry of both. *Proc. Natl. Acad. Sci. U.S.A.* **112**, 4877–4884 (2015).
- T. C. Prang, The African ape-like foot of *Ardipithecus ramidus* and its implications for the origin of bipedalism. *eLife* **8**, e44433 (2019).
- A. Keith, Man's posture: Its evolution and disorders. *Br. Med. J.* **1**, 580 (1923).
- W. K. Gregory, The origin of man from a brachiating anthropoid stock. *Science* **71**, 645–650 (1930).
- A. H. Schultz, The skeleton of the trunk and limbs of higher primates. *Hum. Biol.* **2**, 303–438 (1930).
- J. R. Napier, Studies of the hands of living primates. *Proc. Zool. Soc. Lond.* **134**, 647–657 (1960).
- W. L. Straus, The posture of the great ape hand in locomotion, and its phylogenetic implications. *Am. J. Phys. Anthropol.* **27**, 199–207 (1940).
- W. L. Straus, Rudimentary digits in primates. *Q. Rev. Biol.* **17**, 228–243 (1942).
- W. L. Straus, The riddle of man's ancestry. *Q. Rev. Biol.* **24**, 200–223 (1949).
- A. H. Schultz, Characters common to higher primates and characters specific for man. *Q. Rev. Biol.* **11**, 259–283 (1936).
- O. J. Lewis, Evolutionary change in the primate wrist and inferior radio-ulnar joints. *Anat. Rec.* **151**, 275–285 (1965).
- M. W. Marzke, Origin of the human hand. *Am. J. Phys. Anthropol.* **34**, 61–84 (1971).
- M. Cartmill, K. Milton, The lorisiform wrist joint and the evolution of “brachiating” adaptations in the Hominoidea. *Am. J. Phys. Anthropol.* **47**, 249–272 (1977).
- D. Pilbeam, M. D. Rose, J. C. Barry, S. M. Ibrahim Shah, New *Sivapithecus* humeri from Pakistan and the relationship of *Sivapithecus* and *Pongo*. *Nature* **348**, 237–239 (1990).
- S. Almécija, D. M. Alba, S. Moyà-Solà, M. Köhler, Orang-like manual adaptations in the fossil hominoid *Hispanopithecus laietanus*: First steps towards great ape suspensory behaviours. *Proc. R. Soc. B* **274**, 2375–2384 (2007).
- A. S. Deane, D. R. Begun, *Pierolapithecus* locomotor adaptations: A reply to Alba et al.'s comment on Deane and Begun (2008). *J. Hum. Evol.* **1**, 150–154 (2010).
- M. Böhme, N. Spassov, J. Fuss, A. Tröscher, A. S. Deane, J. Prieto, U. Kirscher, T. Lechner, D. R. Begun, A new Miocene ape and locomotion in the ancestor of great apes and humans. *Nature* **575**, 489–493 (2019).
- S. Almécija, D. M. Alba, S. Moyà-Solà, *Pierolapithecus* and the functional morphology of Miocene ape hand phalanges: Paleobiological and evolutionary implications. *J. Hum. Evol.* **57**, 284–297 (2009).
- S. Almécija, J. B. Smaers, W. L. Jungers, The evolution of human and ape hand proportions. *Nat. Commun.* **6**, 7717 (2015).
- C. Darwin, *Descent of Man: And Selection in Relation to Sex* (J. Murray, 1871).
- S. L. Washburn, Speculations on the interrelations of the history of tools and biological evolution. *Hum. Biol.* **31**, 21–31 (1959).
- D. M. Alba, S. Moyà-Solà, M. Köhler, Morphological affinities of the *Australopithecus afarensis* hand on the basis of manual proportions and relative thumb length. *J. Hum. Evol.* **44**, 225–254 (2003).
- J. G. Fleagle, J. T. Stern, W. L. Jungers, R. L. Susman, A. K. Vangor, J. P. Wells, Climbing: A biomechanical link with brachiation and with bipedalism. *Symp. Zool. Soc. Lond.* **48**, 359–375 (1981).
- D. L. Gebo, Climbing, brachiation, and terrestrial quadrupedalism: Historical precursors of hominid bipedalism. *Am. J. Phys. Anthropol.* **101**, 55–92 (1996).
- C. Rollan, D. E. Lieberman, B. Hallgrímsson, The coevolution of human hands and feet. *Evolution* **64**, 1558–1568 (2010).
- C. Rollan, A. D. Gordon, Reassessing manual proportions in *Australopithecus afarensis*. *Am. J. Phys. Anthropol.* **152**, 393–406 (2013).
- T. L. Kivell, J. M. Kibii, S. E. Churchill, P. Schmid, L. R. Berger, *Australopithecus sediba* hand demonstrates mosaic evolution of locomotor and manipulative abilities. *Science* **333**, 1411–1417 (2011).
- E. E. Sarmiento, Anatomy of the hominoid wrist joint: Its evolutionary and functional implications. *Int. J. Primatol.* **9**, 281–345 (1988).
- N. H. Nyugen, D. Pahr, T. Gross, M. M. Skinner, T. L. Kivell, Micro-finite element modeling of the siamang (*Symphalangus syndactylus*) third proximal phalanx: The functional role of curvature and the flexor sheath ridge. *J. Hum. Evol.* **67**, 60–75 (2014).
- H. Preuschoft, Functional anatomy of the upper extremity. *The Chimpanzee* **6**, 34–120 (1973).
- M. W. Marzke, Tool making, hand morphology and fossil hominins. *Philos. Trans. R. Soc. Lond. B Biol. Sci.* **368**, 20120414 (2013).
- T. L. Kivell, A. S. Deane, M. W. Tocheri, C. M. Orr, P. Schmid, J. Hawks, L. R. Berger, S. E. Churchill, The hand of *Homo naledi*. *Nat. Commun.* **6**, 8431 (2015).
- R. L. Susman, Comparative and functional morphology of hominoid fingers. *Am. J. Phys. Anthropol.* **50**, 215–236 (1979).
- R. L. Susman, J. T. Stern, W. L. Jungers, Arboreality and bipedality in the Hadar hominids. *Folia Primatol.* **43**, 113–156 (1984).
- M. Butler, A. A. King, Phylogenetic comparative analysis: A modeling approach for adaptive evolution. *Am. Nat.* **164**, 683–695 (2004).
- T. Ingram, D. L. Mahler, SURFACE: Detecting convergent evolution from comparative data by fitting Ornstein-Uhlenbeck models with stepwise Akaike Information Criterion. *Meth. Ecol. Evol.* **4**, 416–425 (2013).
- M. Grabowski, W. L. Jungers, Evidence of a chimpanzee-sized ancestor of humans but a gibbon-sized ancestor of apes. *Nat. Commun.* **8**, 880 (2017).
- B. A. Patel, Functional morphology of cercopithecoid primate metacarpals. *J. Hum. Evol.* **58**, 320–337 (2010).
- C. Boettiger, G. Coop, P. Ralph, Is your phylogeny informative? Measuring the power of comparative methods. *Evolution* **66**, 2240–2251 (2012).
- D. C. Adams, M. L. Collyer, Multivariate phylogenetic comparative methods: Evaluations, comparisons, and recommendations. *Syst. Biol.* **67**, 14–31 (2018).
- M. G. Elliot, A. O. Mooers, Inferring ancestral states without assuming neutrality or gradualism using a stable model of continuous character evolution. *BMC Evol. Biol.* **14**, 226 (2014).
- L. J. Revell, `phytools`: An R package for phylogenetic comparative biology (and other things). *Methods Ecol. Evol.* **3**, 217–223 (2012).
- D. Orme, R. Freckleton, G. Thomas, T. Petzoldt, S. Fritz, N. Isaac, W. Pearce, *caper: Comparative Analyses of Phylogenetics and Evolution in R. R package version 1.0.1* (2018); <https://CRAN.R-project.org/package=caper>.
- M. A. Cartmill, Pads and claws in arboreal locomotion, in *Primate Locomotion*, F. A. Jenkins, Ed. (Academic Press, 1974), pp. 45–83.
- R. H. Tuttle, Functional and evolutionary biology of hylobatid hands and feet. *Gibbon Siamang* **1**, 136–206 (1972).
- D. R. Begun, New catarrhine phalanges from Rudabánya (Northeastern Hungary) and the problem of parallelism and convergence in hominoid postcranial morphology. *J. Hum. Evol.* **24**, 373–402 (1993).
- R. H. Tuttle, Quantitative and functional studies on the hands of the anthropoidea. I. The Hominoidea. *J. Morphol.* **128**, 309–363 (1969).
- R. H. Tuttle, Knuckle-walking and the evolution of hominoid hands. *Am. J. Phys. Anthropol.* **26**, 171–206 (1967).

52. S. E. Inuoye, Ontogeny and allometry of African ape manual rays. *J. Hum. Evol.* **23**, 107–138 (1992).
53. S. A. Williams, Variation in anthropoid vertebral formulae: Implications for homology and homoplasy in hominoid evolution. *J. Exp. Zool. B Mol. Dev. Evol.* **318**, 134–147 (2011).
54. N. M. Young, T. D. Capellini, N. T. Roach, Z. Alemseged, Fossil hominin shoulders support an African ape-like last common ancestor of humans and chimpanzees. *Proc. Natl. Acad. Sci. U.S.A.* **112**, 11829–11834 (2015).
55. D. R. Pilbeam, D. E. Lieberman, Reconstructing the last common ancestor of chimpanzees and humans, in *Chimpanzees and Human Evolution*, M.N. Muller, R. W. Wrangham, D. R. Pilbeam, Eds. (Harvard Univ. Press, 2017), pp. 22–141.
56. M. W. Marzke, Precision grips, hand morphology, and tools. *Am. J. Phys. Anthropol.* **102**, 91–110 (1997).
57. M. W. Tocheri, C. M. Orr, M. C. Jacobsky, M. W. Marzke, The evolutionary history of the hominin hand since the last common ancestor of *Pan* and *Homo*. *J. Anat.* **212**, 544–562 (2008).
58. C. V. Ward, M. W. Tocheri, J. M. Plavcan, F. H. Brown, F. K. Manthi, Early Pleistocene third metacarpal from Kenya and the evolution of modern human-like hand morphology. *Proc. Natl. Acad. Sci. U.S.A.* **111**, 121–124 (2014).
59. S. Harmand, J. E. Lewis, C. S. Feibel, C. J. Lepre, S. Prat, A. Lenoble, X. Boës, R. L. Quinn, M. Brenet, A. Arroyo, N. Taylor, S. Clément, G. Daver, J. P. Brugal, L. Leakey, R. A. Mortlock, J. D. Wright, S. Lokorodi, C. Kirwa, D. V. Kent, H. Roche, 3.3-million-year-old stone tools from Lomekwi 3, West Turkana, Kenya. *Nature* **521**, 310–315 (2015).
60. S. P. McPherron, Z. Alemseged, C. W. Marean, J. G. Wynn, D. Reed, D. Geraads, R. Bobe, H. A. Béarat, Evidence for stone-tool-assisted consumption of animal tissues before 3.39 million years ago at Dikika, Ethiopia. *Nature* **466**, 857–860 (2010).
61. J. Napier, Fossil hand bones from Olduvai Gorge. *Nature* **196**, 409–411 (1962).
62. M. W. Marzke, R. F. Marzke, R. L. Linscheid, P. Smutz, B. Steinberg, S. Reece, K. An, Chimpanzee thumb muscle cross sections, moment arms and potential torques, and comparisons with humans. *Am. J. Phys. Anthropol.* **110**, 163–178 (1999).
63. C. Rolian, D. E. Lieberman, J. P. Zermeno, Hand biomechanics during simulated stone tool use. *J. Hum. Evol.* **61**, 26–41 (2011).
64. C. Rolian, S. Carvalho, Tool use and manufacture in the last common ancestor of *Pan* and *Homo*, in *Chimpanzees and Human Evolution*, M. N. Muller, R. W. Wrangham, D. R. Pilbeam, Eds. (Harvard Univ. Press, 2017), pp. 602–644.
65. M. A. Panger, A. S. Brooks, B. G. Richmond, B. Wood, Older than the Oldowan? Rethinking the emergence of hominin tool use. *Evol. Anthropol.* **11**, 235–245 (2002).
66. M. J. Liu, C. H. Xiong, D. Hu, Assessing the manipulative potentials of monkeys, apes and humans from hand proportions: Implications for hand evolution. *Proc. Biol. Sci.* **283**, 20161923 (2016).
67. A. Bardo, L. Vigouroux, T. L. Kivell, E. Pouydebat, The impact of hand proportions on tool grip abilities in humans, great apes and fossil hominins: A biomechanical analysis using musculoskeletal simulation. *J. Hum. Evol.* **125**, 106–121 (2018).
68. M. W. Marzke, Joint functions and grips of the *Australopithecus afarensis* hand, with specific reference to the region of the capitate. *J. Hum. Evol.* **12**, 192–211 (1983).
69. M. Domalain, A. Bertin, G. Daver, Was *Australopithecus afarensis* able to make the Lomekwian stone tools? Towards a realistic biomechanical simulation of hand force capability in fossil hominins and new insights on the role of the fifth digit. *C. R. Palevol* **16**, 572–584 (2017).
70. M. E. Bush, C. O. Lovejoy, D. C. Johanson, Y. Coppens, Hominid carpal, metacarpal, and phalangeal bones recovered from the Hadar formation: 1974–1977 collections. *Am. J. Phys. Anthropol.* **57**, 651–677 (1982).
71. W. H. Kimbel, G. Suwa, B. Asfaw, Y. Rak, T. D. White, *Ardipithecus ramidus* and the evolution of the human cranial base. *Proc. Natl. Acad. Sci. U.S.A.* **111**, 948–953 (2014).
72. E. E. Kozma, N. M. Webb, W. E. H. Harcourt-Smith, D. A. Raichlen, K. D'Aouit, M. H. Brown, E. M. Finestone, S. R. Ross, P. Aerts, H. Pontzer, Hip extensor mechanics and the evolution of walking and climbing capabilities in humans, apes, and fossil hominins. *Proc. Natl. Acad. Sci. U.S.A.* **115**, 4134–4139 (2018).
73. P. J. Fernández, C. S. Mongle, L. Leakey, D. J. Proctor, C. M. Orr, B. A. Patel, S. Almécija, M. W. Tocheri, W. Jungers, Evolution and function of the hominin forefoot. *Proc. Natl. Acad. Sci. U.S.A.* **115**, 8746–8751 (2018).
74. M. D. Leakey, R. L. Hay, Pliocene footprints in the Laetoli Beds at Laetoli, northern Tanzania. *Nature* **278**, 317–323 (1979).
75. B. Latimer, C. O. Lovejoy, Hallucal tarsometatarsal joint in *Australopithecus afarensis*. *Am. J. Phys. Anthropol.* **82**, 125–133 (1990).
76. Y. Haile-Selassie, B. Saylor, A. Deino, N. E. Levin, M. Alene, B. M. Latimer, A new hominin foot from Ethiopia shows multiple Pliocene bipedal adaptations. *Nature* **483**, 565–569 (2012).
77. T. C. Prang, “The Origin and Evolution of Human Bipedalism as Revealed by Foot Morphology,” thesis, New York University, 2019.
78. E. Trinkaus, *The Shanidar Neandertals* (Academic Press, 1983).
79. R. J. Smith, W. L. Jungers, Body mass in comparative primatology. *J. Hum. Evol.* **32**, 532–559 (1997).
80. H. M. Garvin, M. C. Elliott, L. K. Deleze, J. Hawks, S. E. Churchill, L. R. Berger, T. W. Holliday, Body size, brain size, and sexual dimorphism in *Homo naledi* from the Dinaledi Chamber. *J. Hum. Evol.* **111**, 119–138 (2015).
81. M. Grabowski, K. G. Hatala, W. L. Jungers, Body mass estimates of the earliest possible hominins and implications for the last common ancestor. *J. Hum. Evol.* **122**, 84–92 (2018).
82. D. M. Alba, S. Almécija, I. Casanovas-Vilar, J. M. Méndez, S. Moyà-Solà, A partial skeleton of the fossil great ape *Hispanopithecus laietanus* from Can Feu and the mosaic evolution of crown-hominoid positional behaviors. *PLOS ONE* **7**, e39617 (2012).
83. S. Moyà-Solà, M. Köhler, D. M. Alba, I. Casanovas-Vilar, J. Galindo, *Pierolapithecus catalaunicus*, a new Middle Miocene great ape from Spain. *Science* **306**, 1339–1344 (2009).
84. C. Arnold, L. J. Matthews, C. L. Nunn, The 10kTrees website: A new online resource for primate phylogeny. *Evol. Anthropol.* **19**, 114–118 (2010).
85. D. S. Strait, F. E. Grine, Inferring hominoid and early hominid phylogeny using craniodental characters: The role of fossil taxa. *J. Hum. Evol.* **47**, 399–452 (2004).
86. M. Dembo, D. Radović, H. M. Garvin, M. F. Laird, L. Schroeder, J. E. Scott, J. Brophy, R. R. Ackermann, C. M. Musiba, D. J. de Ruiter, A. Ø. Mooers, M. Collard, The evolutionary relationships and age of *Homo naledi*: An assessment using dated Bayesian phylogenetic methods. *J. Hum. Evol.* **97**, 17–26 (2016).
87. G. WoldeGabriel, S. H. Ambrose, D. Barboni, R. Bonnefille, L. Bremond, B. Currie, D. DeGusta, W. K. Hart, A. M. Murray, P. R. Renne, M. C. Jolly-Saad, K. M. Stewart, T. D. White, The geological, isotopic, botanical, invertebrate, and lower vertebrate surroundings of *Ardipithecus ramidus*. *Science* **326**, 65e1–65e5 (2009).
88. R Core Team, *R: A language and environment for statistical computing* (R Foundation for Statistical Computing, Vienna, Austria).
89. S. P. Brooks, A. Gelman, General methods for monitoring convergence of iterative simulations. *J. Comput. Graph. Stat.* **7**, 434–455 (1998).
90. T. Ando, T. Tsay, Predictive likelihood for Bayesian model selection and averaging. *Int. J. Forecast.* **26**, 744–763 (2010).

Acknowledgments: The University of the Witwatersrand, the Evolutionary Studies Institute, B. Zipfel, and S. Jirah provided access to *Au. sediba* and *H. naledi* fossil material in the Phillip V. Tobias Fossil Primate and Hominid Laboratory. E. Westwig (American Museum of Natural History), D. Lunde (U.S. National Museum of Natural History), L. Jellema (Cleveland Museum of Natural History), J. Chupasko (Harvard Museum of Comparative Zoology), curatorial staff at the Field Museum, T. White (Human Evolution Research Center at the University of California, Berkeley), H. Taboada (Center for the Study of Human Origins), C. Conroy (Museum of Vertebrate Zoology at Berkeley), W. Wendelen and E. Gilissen (Royal Museum for Central Africa), and M. Black and N. Johnson (Phoebe A. Hearst Museum of Anthropology at the University of California, Berkeley) provided access to museum specimens. G. Gallo provided assistance with the illustration of stone tools. **Funding:** T.C.P. received a Wenner-Gren Foundation Dissertation Fieldwork grant. **Author contributions:** T.C.P. and K.R. collected the data, T.C.P. performed the analyses with contributions from M.G., and T.C.P. wrote the manuscript with contributions from K.R., M.G., and S.A.W. **Competing interests:** The authors declare that they have no competing interests. **Data and materials availability:** All data needed to evaluate the conclusions in the paper are available on the Dryad digital data repository (<https://doi.org/10.5061/dryad.tmpg4f4x7>). Additional data related to this paper may be requested from the authors.

Submitted 13 October 2020

Accepted 12 January 2021

Published 24 February 2021

10.1126/sciadv.abf2474

Citation: T. C. Prang, K. Ramirez, M. Grabowski, S. A. Williams, *Ardipithecus* hand provides evidence that humans and chimpanzees evolved from an ancestor with suspensory adaptations. *Sci. Adv.* **7**, eabf2474 (2021).

***Ardipithecus* hand provides evidence that humans and chimpanzees evolved from an ancestor with suspensory adaptations**

Thomas C. Prang, Kristen Ramirez, Mark Grabowski and Scott A. Williams

Sci Adv 7 (9), eabf2474.
DOI: 10.1126/sciadv.abf2474

ARTICLE TOOLS	http://advances.sciencemag.org/content/7/9/eabf2474
SUPPLEMENTARY MATERIALS	http://advances.sciencemag.org/content/suppl/2021/02/22/7.9.eabf2474.DC1
REFERENCES	This article cites 82 articles, 8 of which you can access for free http://advances.sciencemag.org/content/7/9/eabf2474#BIBL
PERMISSIONS	http://www.sciencemag.org/help/reprints-and-permissions

Use of this article is subject to the [Terms of Service](#)

Science Advances (ISSN 2375-2548) is published by the American Association for the Advancement of Science, 1200 New York Avenue NW, Washington, DC 20005. The title *Science Advances* is a registered trademark of AAAS.

Copyright © 2021 The Authors, some rights reserved; exclusive licensee American Association for the Advancement of Science. No claim to original U.S. Government Works. Distributed under a Creative Commons Attribution NonCommercial License 4.0 (CC BY-NC).